



## Imaging an hyperpicnal turbidite outcrop in Almada Basin (Brazil)

Marco A. R. Ceia, A. Abel G. Carrasquilla, UENF/LENEP & Jandyr M. Travassos MCT/ON

Copyright 2005, SBGf - Sociedade Brasileira de Geofísica

This paper was prepared for presentation at the 9<sup>th</sup> International Congress of the Brazilian Geophysical Society held in Salvador, Brazil, 11-14 September 2005.

Contents of this paper were reviewed by the Technical Committee of the 9<sup>th</sup> International Congress of the Brazilian Geophysical Society. Ideas and concepts of the text are authors' responsibility and do not necessarily represent any position of the SBGf, its officers or members. Electronic reproduction or storage of any part of this paper for commercial purposes without the written consent of the Brazilian Geophysical Society is prohibited.

### Abstract

In onshore Almada Basin, northeast Brazil, sandy and/or conglomeratic turbidites and shales outcrops of Urucutuca Formation occur. These rocks are part of an exhumed portion of the filling-section of the Almada Canyon, which is well mapped by seismic studies in offshore part. Such outcrops are unique examples of passive margin transgressive marine sequence turbidites in Brazil, which were sedimented during the Maastrichtian/Campanian. They are analogous to some important turbidite reservoirs of Campos basin, the main Brazilian petroleum basin. In this work, a set of geo-radar (GPR) profiles was measured at an outcrop in Almada Basin. The dataset, after a selective processing flow, released high resolution images, that allied to 3D visualization resources and geological interpretations of the exposed section and cores obtained in a nearby well, could help to delineate several subsurface structures like channels and interfaces between different lithologies. Furthermore, it was possible to evaluate the relative electric permittivity from the GPR signal, and using forward modelling algorithms, to test some electrical conductivity values, in such a way it was possible to provide a geophysical characterization of that exposed section. These information aims to be useful for designing more detailed stratigraphical models, that can improve the knowledge of analogous turbidite reservoirs and afterward aid to enhance the production on oilfields associated to this kind of reservoirs.

### Introduction

Turbidite reservoirs are the most important type of petroleum reservoirs in Brazil, mainly in Campos Basin, the largest Brazilian oil producer basin. Because many of the geological features likely to control production from turbidite reservoirs are smaller than the resolution from even the highest quality seismic reflection surveys, it is necessary to add information of equivalent outcrops on land to the seismic model of such reservoirs, in order to produce accurate porosity and permeability models of them (Young et al., 1999; Young et al., 2001). The information from reservoir analogues can lead to new discoveries and to enhance oil recovery by a better well location strategy.

The absence of turbidite outcrops in the on shore portion of Campos Basin lead us to study Almada Basin turbidite outcrops, which are contemporaneous and geologically similar to some important Campos Basin

channelized turbidites, as found in Pargo and Carapeba Fields.

On the other hand, the GPR method has been widely used for high resolution imaging of internal structure of reservoir analogs (Young et al, 2001) due to its sub-meter resolution, which can reveal several stratigraphical features. This paper shows GPR images obtained at one of the Almada Basin outcrops and their interpretation through the comparison to the exposed section geology and forward modelling of the GPR data.

Regarding geological framework, Almada Basin is a passive margin basin in north-east coast of Brazil, between 14° 15' S and 14° 55' S. It's bounded by the Itacaré High, at north, and by the Olivença High, at south. It also comprises a small on shore portion, which spreads over 200 km<sup>2</sup> with a maximum sedimentary coverage of 1800 m. The offshore portion is larger, spreading over roughly 1300 km<sup>2</sup> until a bathymetric level of 200 m, with a maximum sedimentary coverage larger than 6000 m.

Early detailed geological mapping of on shore portion was done in 1963 (Carvalho, 1965). In this portion, sandy and/or conglomeratic turbidites and planctonic foraminiferous shales outcrop. These geological features are related to Urucutuca Formation (Mesozoic/Upper Cretaceous) and are an exhumed part of the filling-section of the Almada Canyon, a huge erosive feature, which is seismically well defined in offshore portion. These rocks are analogues to other formations founded in Campos, Espírito Santo and Cumuruxatiba basins, in Brazil.

Detailed studies of the outcrops can be found in Bruhn & Moraes (1989) and Mendes (1998). Figure 1 shows the main Urucutuca Formation channeling turbidite outcrops location (Bruhn & Moraes, 1989). In this paper we restrict ourselves to outcrop 2A (Figure 2). A scientific project called "Turbiditos" (Dias et al., 2004), provide new geological and geophysical datasets, which lead to new stratigraphical and structural interpretation of that on shore portion. According to the geological interpretation of "Turbiditos" project, Almada Canyon origin is possibly related to the movement of ancient faults of the basement during the Cretaceous, which produced weak zones that conditioned sub-aerial and submarine erosion and the collection of the region's fluvial systems. Initially those faults acted as strike-slip faults, but during the deposition of Urucutuca Formation they were re-activated as normal (gravity) faults, creating a submarine conduct which spreaded from the continent, where possibly bounded a river mouth among the mountains, until the deepwater portion. That submarine depression received several fluvial discharges, which created flows and hyperpicnal floods that ran through the canyon as turbidity currents, leading to substrata erosion and carrying a huge volume of sediments from the basin. Those sediments are called hyperpicnal turbidites (d'Ávila et al., 2004).

### Methodology

Ground penetrating radar (GPR), also known as geo-radar, has become, in recent years, a popular geophysical technique to study shallow subsurface sediments, as it allows for fast acquisition of high-resolution images of the sedimentary architecture. GPR is based on the reflections of electromagnetic waves, transmitted from a point at the surface through the subsurface. These reflections are caused by changes in the electromagnetic properties of subsurface features, that can be associated to changes in lithology or variation in the water content. Good references for this method can be found in Annan (1992) and Davis & Annan (1989).

The field survey was carried out in 3 outcrops near Ilhéus, northeast of Brazil (Figure 1). In this work, we will restrict ourselves to the profiles acquired on the most important outcrop, named 2A. We have done 5 GPR fixed-offset profiles in outcrop 2A. A single common mid-point profile also was carried out for velocity estimation purposes.

We have used a Sensors & Software Inc. PulseEKKO IV system, operating with 100 MHz antennas. Time window and station spacing were set to 300 ns and 0.25 m respectively. Distance between antennas was fixed in 1m. Geographic information was obtained using a Trimble DGPS system and a clinometer to provide a relative topography between GPS points. The CMP profile was also done with steps of 0.2 m (Ceia et al. 2004).

The processing sequence applied to the outcrop 2A dataset consist of: Trace Editing, Dewow, Time-zero Correction, Time-window Limitation, Velocity Analysis, Stolt  $f$ - $k$  Migration, Band-Pass Time Filtering, Elevation Correction.

Velocity information was obtained with CMP profiles and NMO reflection hyperbole semblance. From semblance velocity plots we obtained velocity models for outcrop 2A (Table 1). Those models were used for Stolt Migration. Elevation correction was done using a constant velocity of 0.1 m/ns. A band-pass filter with 30-70-180-500 MHz cutoff frequencies was applied in order to eliminate unwanted noise mainly at low frequencies. The maximum penetration depth in those outcrops were ~15m (Ceia et al. 2004).

Time (ns)	Velocity (m/ns)
$t \leq 50$	0,100
$t > 50$	0,200

Table 1 – Velocity model obtained from semblance analysis of the CMP profile carried on outcrop 2A.

### Discussion and Results

Initially an interpretation was done through the association between the reflectors observed in the radargrams, the geological interpretation of the exposed section (rectangle in Figure 3) and cores obtained in a nearby well (SST-1). Figure 3 shows a summary of the structures observed at this outcrop. Although 3 channels were identified by the radargrams, one of these channels was confirmed by the geological interpretation (d'Ávila et al., 2004) of the exposed sediments (on the center of the figure), which reported two main lithologies: conglomerates and heterolithes (thick sandstones with

thin shale bedding). This channel has roughly 9 m depth and a 54 m width. Its traverse axis is NE-SW. Inner onlap stratification can be seen in this channel. According to d'Ávila et al. (2004), those fine-grain sediments were also reshaped by tides.

Using the velocities described in Table 1, it was possible to estimate relative permittivity values through Equation 1.

$$\epsilon_r = \sqrt{\frac{c}{v}}, \quad (1)$$

where:

$\epsilon_r$  = electric relative permittivity,

$c$  = light speed,

$v$  = velocity of EM waves in a certain medium.

The values founded were 9, that probably is associated to the heterolithes (silt, clay and sandstone), and 2.25 that is probably associated to gravely high density turbidites (coarse sandstone and conglomerates), but such low values can indicate either air waves influence on CMP soundings or the presence of petroleum in the sediments. In fact, traces of petroleum were founded in drill cuttings in a well 5 m ahead from the SST-1 (Lima, 2005), but deeper than the GPR maximum penetration. This way, air waves supposition seems to be more reasonable.

Using the geological interpretation showed in Figure 2 and the information form the radargrams, we built a framework to be used as input for 2D forward modelling algorithm (Giannopoulos, 2002). That algorithm is based on finite difference time domain (FDTD) method, whose approach to the numerical solution of Maxwell's equations is to discretize both the space and time continua. It allows model building derived from simple geometric shapes as rectangles, circles and triangles, such a way that the combinations of those shapes can reproduce some complex geological models. To reduce computational requirements, some suppositions are assumed by GPRMAX2D algorithm in order to simplify the models, like:

- All media (layers) are considered to be linear and isotropic.
- The GPR transmitting antenna is modelled as a line source.
- The constitutive parameters are, in most cases, assumed not to vary with frequency.

The parameters choice was the key step for model building. The area was chosen as a rectangle with 21 m width and 13 m high, based on an outcrop photograph showed in Figure 2. DC relative permittivity values were based in Annan (1992) tables and from those derived from CMP analysis. Conductivities values were based in Annan (1992).

A constant offset was chosen, with 1 m separation. Spatial step size (along the profile) was chosen to be 0.25 m. A Gaussian type pulse with 100 MHz central frequency were also chosen. All of that to simulate the conditions of the GPR profiles carried out on outcrop 2A, such a way we can compare the forward modelling results to the real data.

After several tests, we found the synthetic model showed in Figure 4, which produce a synthetic radargram (Figure 5), that was the best reproduction of the GPR data showed in Figure 6. Only the amplitude calculated from vertical electrical field ( $E_z$ ) is showed. The values used in the final synthetic model are shown in Table 2.

The comparison show that the synthetic model can reproduce the main features displayed in Figure 6. Differences can be due to the variation of electrical properties of the rocks of the same lithology (ex. Water content variation) or to an even more complex layering geometry.

Lithology	Relative Permittivity	Conductivity (mS/m)
Free Air	1.0	0
Shale	11.0	6
Sandstone	6.0	0.1
Conglomerate	4.0	0.05

Table 2 – Relative Permittivity and Conductivity values used for the synthetic model showed in Figure 4.

### Conclusions

The GPR method has been successful revealing some stratigraphic features on Almada basin turbidite outcrops, like channels and layering pattern. GPR images show good agreement to geological interpretation of the exposed section. Heterolithes (thick sandstones with thin shale bedding) and conglomerates were the two main lithologies reported by geological studies. Relative permittivity values were estimated from the velocities obtained in the CMP analysis, but some low values founded, indicates that air waves had influenced CMP analysis. A 2D forward modeling was used to provide conductivity and values. It also helped to improve relative permittivity estimations.

### Acknowledgments

The research leading for this paper was funding by CTPETRO. M.A.R.C. thanks ANP (Brazilian Petroleum Agency) PRH-20 by the doctorate scholarship. J.M.T. and A.A.G.C. thank CNPq by scientific grants. We also would like to thank Carlos A. Dias and Roberto d'Ávila ("Turbiditos" project coordinators) for their support.

### References

- ANNAN, P.; 1992. Ground Penetrating Radar workshop notes: Sensors & Software Inc.
- BRUHN, C. & MORAES, M.; 1989. Turbiditos da Formação Urucutuca na Bacia de Almada, Bahia: um Laboratório de Campo para Estudo de Reservatórios Canalizados. *B Geoci. PETROBRÁS*, 3 (3): 235-267, jul/set. In portuguese.
- CARRALHO, K. W. B. 1965. Geologia da Bacia Sedimentar do Rio Almada. *Boletim Técnico da PETROBRÁS*, Rio de Janeiro, 8 (1):5-55, jan/mar. In portuguese.
- CEIA, M., CARRASQUILLA, A. & TRAVASSOS J.; 2004. Levantamento GPR Afloramentos Turbidíticos da Bacia de Almada (BA). *Revista Brasileira de Geociências*. Vol. 34 (3), pags: 411-418. In portuguese.
- D'ÁVILA R.S.F., SOUZA-CRUZ C.E., OLIVEIRA FILHO, J.S.O., MENEZES, C., CESERO, P., DIAS FILHO, D.C., LIMA, C.C., QUEIROZ, C.L., SANTOS, S.F. & FERREIRA, E.A., 2004. Fácies e Modelo Depositional do Canyon de Almada. in: (Eds) Dias, C.A., Thomaz Filho, A. e D'Ávila, R.S.F., UENF/UERJ. Relatório Final apresentado à FINEP/CTPETRO – PETROBRAS e FAPERJ, projeto "Turbiditos de Almada". Section II/2. In portuguese.
- DAVIS, J.L. & ANNAN A.P., 1989. Ground-Penetrating radar for high-resolution mapping of soil and rock stratigraphy: *Geophys. Prosp.*, **37**, 531-551.
- DIAS C.A., 2004. in: (Eds) Dias, C.A., Thomaz Filho, A. E D'Ávila, R.S.F., UENF/UERJ. Relatório Final apresentado à FINEP/CTPETRO – PETROBRAS e FAPERJ, projeto "Turbiditos de Almada". In portuguese.
- GIANNOPOULOS, A. 2002. GPRMAX2D User's Guide. School of Civil and Environmental Engineering, University of Edinburgh, Scotland, UK.
- LIMA, K.T., 2005. Personal Communication.
- MENDES, M. P.; 1998. Evolução, análise estratigráfica e sistemas turbidíticos em paleocânions submarinos: exemplos de Almada (BA) e Regência (ES). Dissertação de Mestrado, UFRGS, Porto Alegre, 229 pp. In portuguese.
- YOUNG, R. A., PETERSON, B., SLATT, R. M.; 1999. Imaging of Turbidite Outcrop Analogs Using Ground Penetrating Radar. 69th Annual Meeting: Soc. Of Expl. Geophys., 429-432.
- YOUNG, R.A., STAGGS, J., SLATT, R.M., HURLEY, N.F.; 2001. Turbidite Outcrop 3-D Ground Penetrating Radar Imaging: Lewis Shale, WY. 71st Annual Meeting: Soc. of Expl. Geophys., 1592-1595.

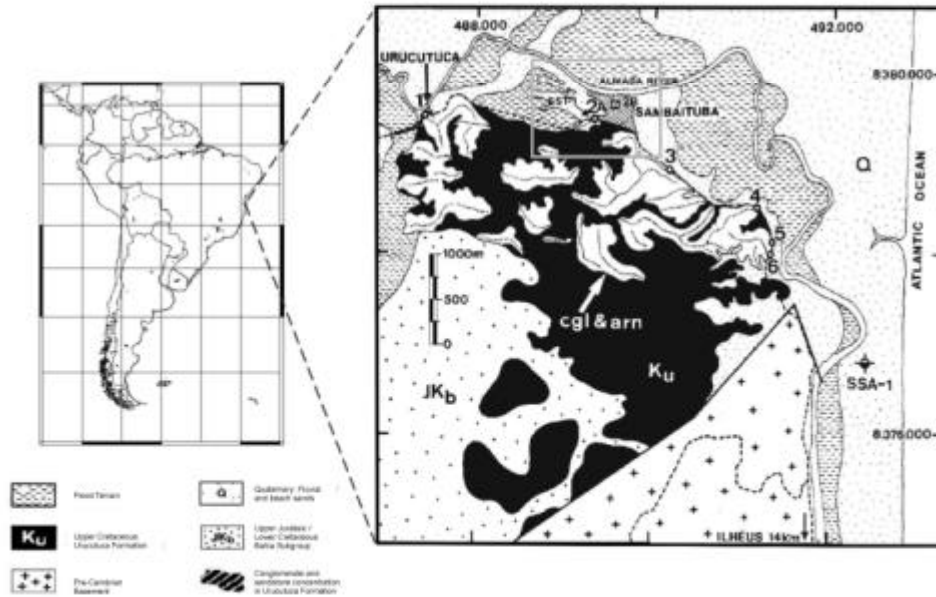


Figure 1 – Map showing the location of the studied area. After Bruhn & Moraes (1989).

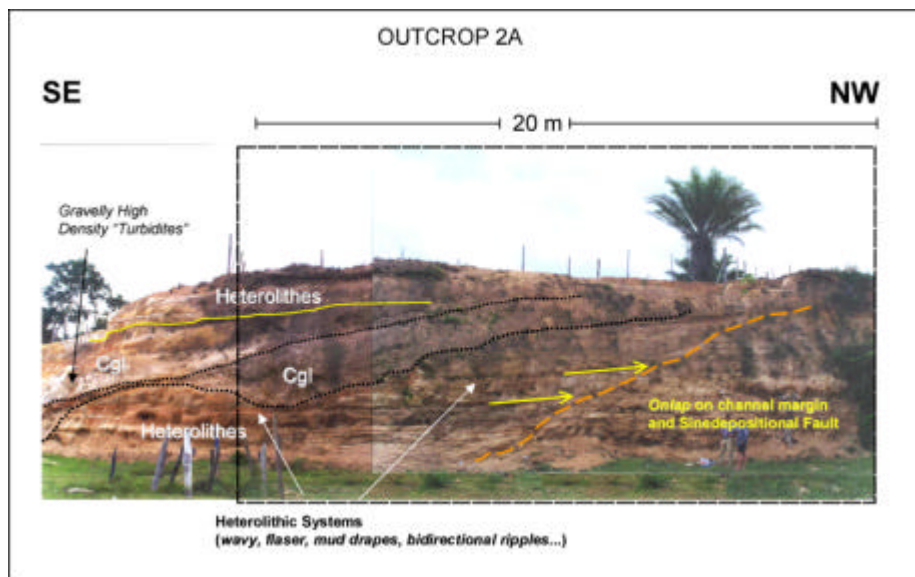


Figure 2 – Outcrop 2A photograph. After d'Ávila et al. (2004).

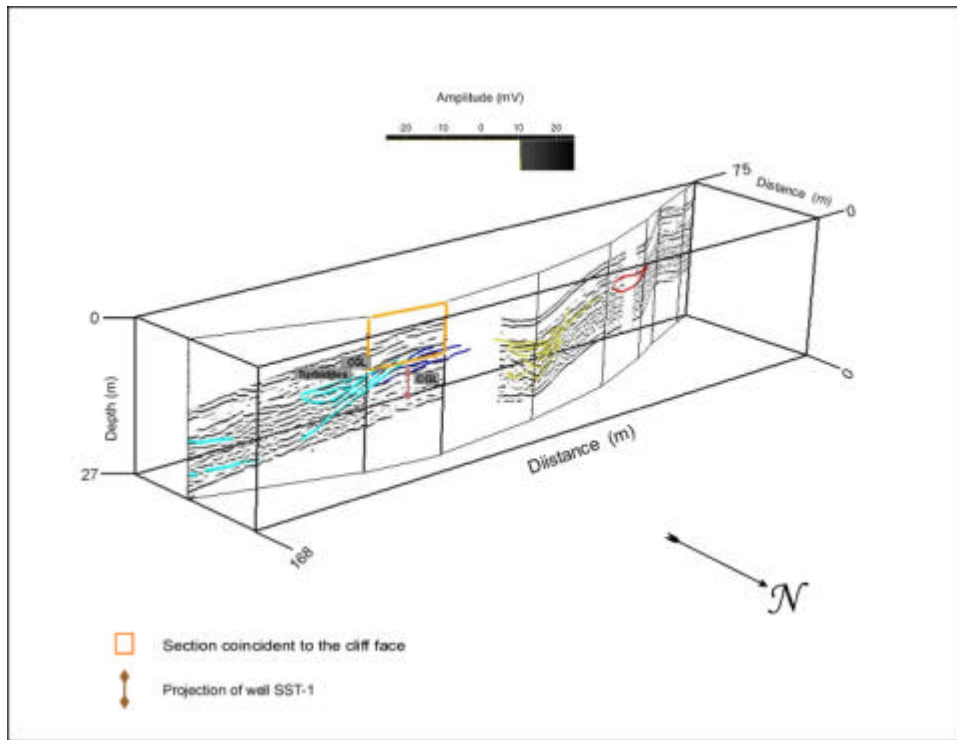


Figure 3 - Summary of the structures observed on outcrop 2A. After Ceia et al. (2004).

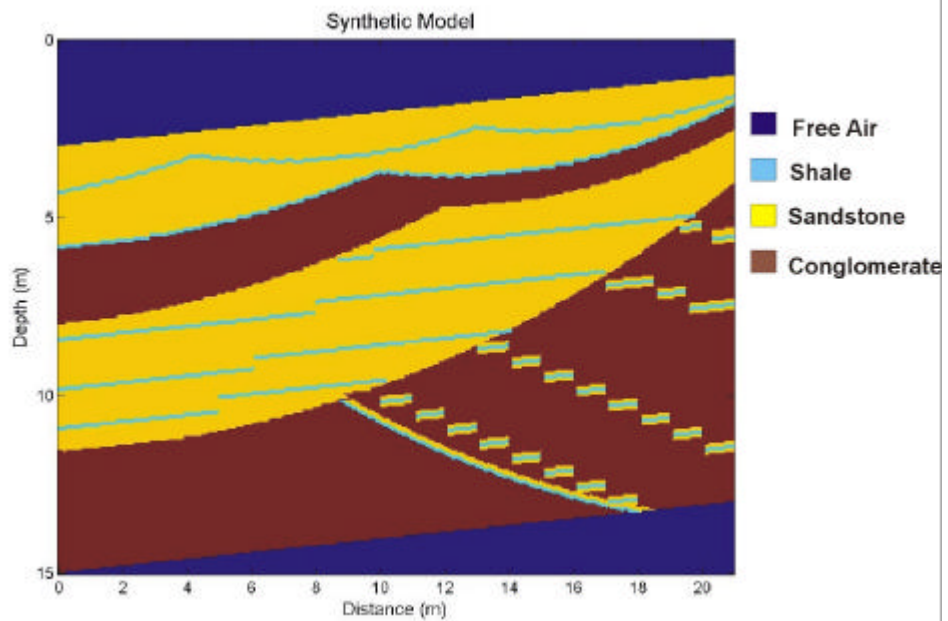


Figure 4 – Synthetic model of a section of outcrop 2A showed in Figure 2.

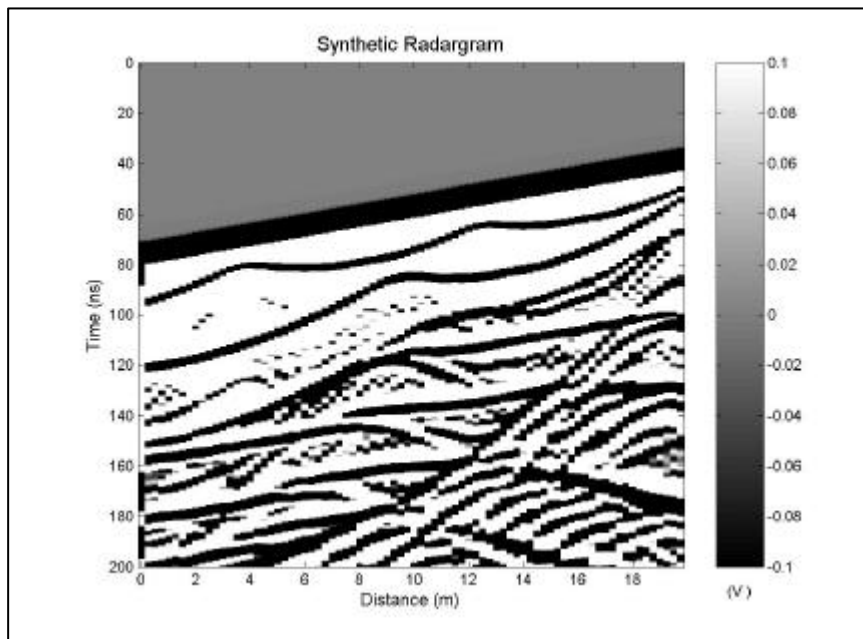


Figure 5 – Synthetic radargram of the model showed in Figure 4.

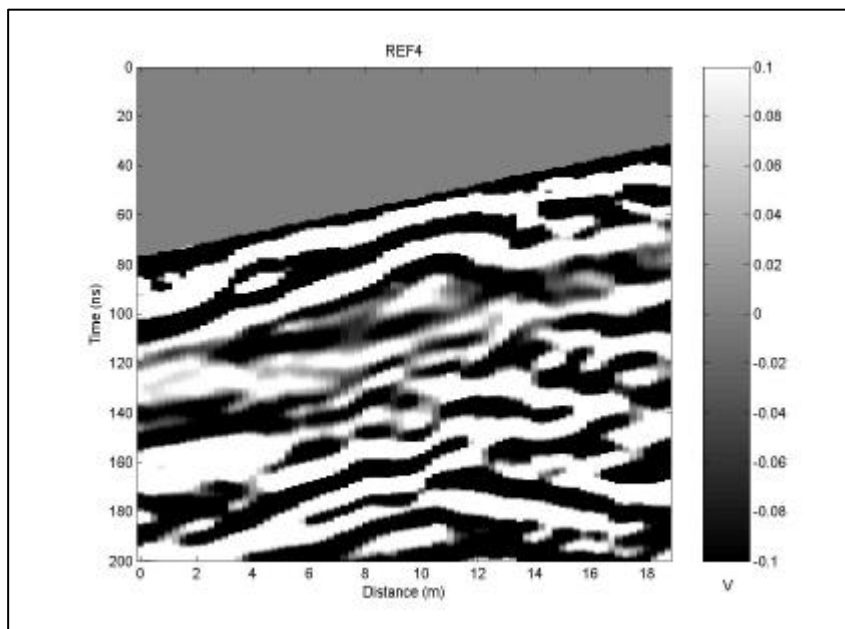


Figure 6 – Radargram of a GPR profile carried on the section of outcrop 2A showed in Figure 2.